Histone Acetyltransferase hALP and Nuclear Membrane Protein hsSUN1 Function in De-condensation of Mitotic Chromosomes

Ya-Hui Chi, Kerstin Haller, Jean-Marie Peloponese, Kuan-Teh Jeang

THE JOURNAL OF BIOLOGICAL CHEMISTRY VOL. 282, NO. 37, pp. 27447–27458, September 14, 2007
Printed in the U.S.A.

Histone Acetyltransferase hALP and Nuclear Membrane Protein hsSUN1 Function in De-condensation of Mitotic Chromosomes*[S]

Received for publication, April 12, 2007, and in revised form, June 21, 2007 Published, JBC Papers in Press, July 13, 2007, DOI 10.1074/jbc.M703098200

Ya-Hui Chi, Kerstin Haller, Jean-Marie Peloponese, Jr., and Kuan-Teh Jeang[1]

From the Molecular Virology Section, Laboratory of Molecular Microbiology, NIAID, National Institutes of Health, Bethesda, Maryland 20892

Replicated mammalian chromosomes condense to segregate during anaphase, and they de-condense at the conclusion of mitosis. Currently, it is not understood what the factors and events are that specify de-condensation. Here, we demonstrate that chromosome de-condensation needs the function of an inner nuclear membrane (INM) protein hsSUN1 and a membrane-associated histone acetyltransferase (HAT), hALP. We propose that nascently reforming nuclear envelope employs hsSUN1 and hALP to acetylate histones for de-compacting DNA at the end of mitosis.

The eukaryotic nucleus is separated from other organelles by an envelope containing two membrane layers continuous with the endoplasmic reticulum. Nuclear membrane proteins fall into three categories according to their localization. The first group is the trans-nuclear membrane proteins resident in the nuclear pore complex (NPC).[2] The second group contains the inner membrane proteins (INM), which include the lamin B receptor (LBR), emerin, and lamin-associated polypeptides (LAPs). The third group includes proteins underlying the nuclear membrane such as nuclear lamina (1). Functionally, the INM provides a physical barrier; the NPC serves for the transport of material between the nucleus and the cytoplasm (2); and the nuclear lamina erects a meshwork, which maintains nuclear structure and assists indirectly in DNA replication and RNA processing (3, 4).

Most INM proteins are associated with the nuclear lamina. In a proteomic study of INM proteins, in addition to 13 known proteins, 67 uncharacterized open reading frames (ORFs) were identified (5). 23 of these ORFs map to chromosome regions linked to a variety of dystrophies collectively termed "nuclear envelopathies" (5). These diseases have phenotypes ranging from cardiac and skeletal myopathies, lipodystrophy, peripheral neuropathy, and premature aging (6–9). Genetic studies have associated mutations in emerin, lamin A/C, and lamin B receptor with such pathologies (7, 9). An emerging notion is that the INM proteins are needed to maintain nuclear integrity and guard against mechanical stress (10–12). Plausibly, then, tissues that experience high mechanical stress may have increased sensitivity to the consequence of mutated INM proteins. Nonetheless, a fuller understanding of how abnormalities in nuclear membrane contribute to pathogenesis remains to be elucidated.

Some INM proteins have a Sad1-UNC84 (SUN) domain at their C termini (13). The SUN domain was first identified based on the sequence alignment of Sad1 of *Schizosaccharomyces pombe* and UNC-84 of *Caenorhabditis elegans* (14). All SUN proteins contain putative transmembrane regions, suggesting that they localize to membranes at some periods during the cell cycle. Curiously, steady state *S. pombe* Sad1 predominates at spindle pole bodies and has been inferred to function in the formation of the mitotic spindle (15); on the other hand, UNC-84 localizes in the *C. elegans* nuclear envelope (16). Mammals have four SUN proteins, SUN1 (also called UNC84A), SUN2 (also called UN84B), a sperm-associated antigen 4-like (SPAG4) protein, and a hypothetical protein, MGC33329. To date, other than a described ability to bind nesprin-2 (17, 18), little else is known about the function of mammalian SUN proteins (18–21).

Because the timing of nuclear membrane reformation at the end of mitosis appears to be linked to chromosome de-condensation, we have characterized here the mitotic role for hsSUN1. We find that hsSUN1 is one of the earliest INM factors to associate with segregated daughter chromosomes in anaphase. Knockdown of hsSUN1 leads to hypoacetylated histones and delayed de-condensation of chromosomes at the end of mitosis. A HAT protein, hALP, previously reported to be associated with mammalian inner nuclear membrane (5), was found to bind hsSUN1 and to be required for proper mitotic chromosome de-condensation. Our findings broach a mechanism used by nascently enveloped daughter nuclei to de-compact chromosomes, preparing them for gene expression in the impending interphase.

* The costs of publication of this article were defrayed in part by the payment of page charges. This article must therefore be hereby marked "*advertisement*" in accordance with 18 U.S.C. Section 1734 solely to indicate this fact.

[S] The on-line version of this article (available at http://www.jbc.org) contains supplemental Fig. S1 and movie 1.

[1] To whom correspondence should be addressed: Bldg. 4, Rm. 306, 9000 Rockville Pike, Bethesda, MD 20892-0460. Tel.: 301-496-6680; Fax: 301-480-3686; E-mail: kj7e@nih.gov.

[2] The abbreviations used are: NPC, nuclear pore complex; SUN, Sad1-UNC84; ChIP, chromatin immunoprecipitation; INM, inner nuclear membrane; H3pSer10, phosphorylated histone H3 at serine 10; hALP, human acetyltransferase-like protein; LAP, lamin-associated polypeptide; LBR, lamin B receptor; HAT, histone acetyltransferase; HDAC, histone deacetylase; ORF, open reading frame; RIPA, radioimmune precipitation assay buffer; PBS, phosphate-buffered saline; GST, glutathione *S*-transferase; HA, hemagglutinin; DAPI, 4′,6-diamidino-2-phenylindole; GFP, green fluorescent protein; WT, wild type.

EXPERIMENTAL PROCEDURES

Plasmid Construction—HsSUN1 (KIAA0810) and hALP cDNA (KIAA1709) were from the Kazusa DNA Research Institute (22). Full-length hsSUN1 (amino acids 1–785) was amplified from the KIAA0810 (hk05647s1) clone using PCR and ligated into pCDNA3.1+ vector (Invitrogen). HA-tagged full-length hsSUN1 and N- and C-terminal deletion mutants (amino acids 1–581, 1–479, 1–377, 1–238, 40–173, 103–785, 205–785, 307–785, 501–785) were constructed by amplifying the indicated sequences by PCR and cloning into pCDNA3.1+ vector. Full-length hALP (amino acids 1–1025, clone fj18302) was amplified by PCR and tagged with FLAG for detection purposes.

Anti-hsSUN1 Antibody Preparation—HsSUN1 amino acids 362–785 were expressed in the pGEX5x-2 vector (Amersham Biosciences). Recombinant GST-fused hsSUN1-(362–785) protein was used for rabbit immunization (Spring Valley Laboratories). Rabbit hsSUN1 antiserum (αhsSUN1-C) was first captured with protein A-agarose (Bio-Rad), and then affinity-purified using GST-hsSUN1-(362–785) fusion protein conjugated to Affi-Gel15 (Bio-Rad).

Western Blotting—HeLa cells were maintained in Dulbecco's modified Eagle's medium containing 10% fetal bovine serum and supplemented with 2 mM L-glutamine and antibiotics. Cells were washed twice with phosphate-buffered saline (PBS), scraped from the culture plate, pelleted, and lysed with RIPA buffer (50 mM HEPES, pH 7.3, 150 mM NaCl, 2 mM EDTA, 20 mM β-glycerophosphate, 0.1 mM Na_3VO_4, 1 mM NaF, 0.5 mM dithiothreitol, and protease inhibitor mixture (Roche Applied Sciences)) containing 1% SDS. For the peptide competition assay, total cell lysates were analyzed by 8% sodium dodecyl sulfate-polyacrylamide gel electrophoresis (SDS-PAGE), transferred to polyvinylidene fluoride membrane, and subjected to immunoblotting. Affinity-purified anti-hsSUN1 was either preincubated with GST-agarose, GST-agarose plus 100 μl of purified GST (400 μg/ml), or GST-agarose plus GST-hsSUN1-(362–785) fusion protein (300 μg/ml, 50 and 200 μl, respectively). Antibodies after incubation with/without GST-agarose plus GST or GST-hsSUN1 fusion proteins were then added to polyvinylidene difluoride membranes blocked with 0.2% I-Block (Tropix) in PBS and 0.1% Tween-20 (Bio-Rad). Alkaline phosphatase-conjugated anti-rabbit secondary antibody was added, and the blots were developed by chemiluminescence following the manufacturer's protocol (Tropix).

Chromatin Association Assay—The chromatin association assay was performed by modifying the chromatin immunoprecipitation (ChIP) protocol described by Upstate. Briefly, cells were transfected with plasmids using Lipofectamine (Invitrogen). 24 h later, cells were cross-linked by adding 1% formaldehyde to the medium and incubated for 10 min at room temperature. The cross-linking reaction was quenched by addition of 0.125 M glycine and incubation at room temperature for another 10 min. Cells were washed with cold PBS, scraped, and pelleted by centrifugation. To extract soluble chromatin and its associated proteins, cells were lysed in SDS-lysis buffer (1% SDS, 50 mM Tris-HCl, pH 8.0, 10 mM EDTA, and protease inhibitor mixture) and sonicated for 5 times for 10-s pulses (Branson, Sonifier, Model 450) and incubated on ice inbetween. Lysates were centrifuged at 12,000 × *g* at 4 °C for 10 min. Soluble fractions of cell lysates were diluted 50 times in RIPA buffer (as described in Western blotting) and incubated with monoclonal anti-HA or anti-FLAG agarose (Sigma-Aldrich) for 16 h at 4 °C. The agarose beads were washed five times with RIPA buffer. Before analyzing the samples with SDS-PAGE, samples were boiled in one volume of 2× Laemmli loading buffer (2% SDS, 20% glycerol, 120 mM Tris-HCl, pH 6.8, 200 mM dithiothreitol, bromphenol blue) for 30 min to reverse the cross-linking.

Immunofluorescence and Confocal Microscopy—Cells were fixed in 4% paraformaldehyde for 20 min at room temperature and permeabilized with 0.1% Triton X-100 in PBS for 5 min at room temperature. To block nonspecific binding, cells were incubated with 1% bovine serum albumin in PBS for 30 min. Antibodies against hsSUN1, emerin (Santa Cruz Biotechnology), lamin B (Santa Cruz Biotechnology), nuclear pore complex (mab414, Covance), α-tubulin (Sigma-Aldrich), CENP-A (MBL) and anti-LAP2 (Sigma-Aldrich), anti-LBR (Epitomics) were added to cells at dilutions of 1:200 to 1:2000 and incubated for 1 h at room temperature. Cells were washed three times with PBS and then probed with fluorescent (Alexa-488, Alexa-594, or Alexa-647)-conjugated secondary antibodies. Cell nuclei were stained with DAPI (Molecular Probes). Cells on the coverslips were mounted on glass slides with antifade reagents (Molecular Probes). Slides were monitored using a Leica TCS-NP/SP confocal microscope. For time-lapse confocal microscopy, live cells were incubated at 37 °C in a humidified Pe-Con environmental chamber supplied with 5% CO_2.

RNAi—Synthetic siRNA duplexes targeting hsSUN1 (5′-CCAUCCUGAGUAUACCUGUCUGUAU-3′) and hALP (5′-CGGCCUUCAGUGCUGUGGUGUUAUA-3′) were from Invitrogen. HeLa cells were transfected with hsSUN1 RNAi using TransMessenger transfection reagent (Qiagen). A GFP-expressing plasmid (Clontech) was co-transfected with hsSUN1 RNAi to monitor transfection efficiency. We also employed unrelated siRNAs with the same GC content as controls. 24–72 h after transfection, cells were analyzed by Western blotting or confocal microscopy.

RESULTS

Determinants of hsSUN1 Localization to the Nuclear Envelope—HsSUN1 was initially described to contain 824 amino acids (13). However, various lengths (ranging from 909 to 974 amino acids) for SUN1 (UNC84A) have been suggested (17, 18, 20, 21, 23, 24). Updated sequencings (KIAA0810, clone hk05647s1) from Kazusa DNA Research Institute and from our own cloning of cDNAs (data not shown) from several human cells (Jurkat, HeLa, and primary human lymphoblastoid cells) reveal that hsSUN1 is 785 amino acids in length. At its C terminus, hsSUN1 conserves with *C. elegans* UNC-84 a 190-amino acid SUN domain (Fig. 1*A*). *In silico* analyses indicate that hsSUN1 has three transmembrane regions located at amino acids 239–256, 263–282, and 289–306; and two coiled-coils at positions 377–402 and 428–466 (Fig. 1*A*).

Evidence supports that hsSUN1 is an INM protein. However, published reports do not agree on which hsSUN1 domain spec-

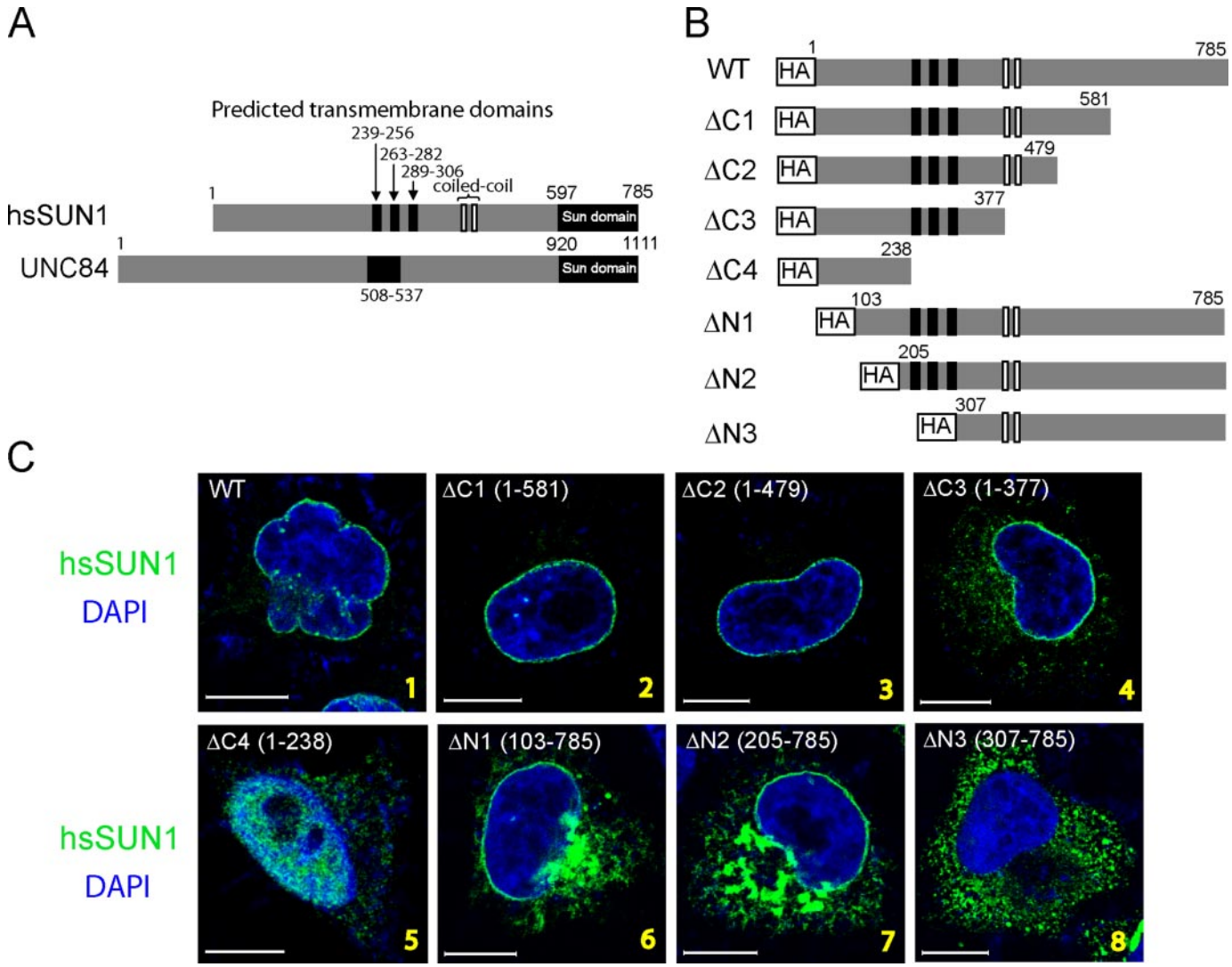

FIGURE 1. **Characterization of hsSUN1 domains for localization in nuclear envelope.** *A*, alignment of hsSUN1 and UNC-84 from *C. elegans* shows a homologous C-terminal SUN domain. HsSUN1 is predicted to have three transmembrane domains in amino acids 239–256, 263–282, and 289–306, respectively. By comparison, UNC-84 has one predicted transmembrane domain (amino acids 508–537). Two coiled-coil domains (amino acids 377–402 and 428–466) are predicted for hsSUN1. *B*, schematic representation of hsSUN1 and its deletion mutants. Transmembrane and coiled-coil domains are labeled as in *A*. *C*, localization of C- and N-terminal deletion mutants (amino acids 1–581, 1–479, 1–377, 1–238, 103–785, 205–785, and 307–785) of hsSUN1 (*green*) in HeLa cells were monitored by immunofluorescence. DNA was stained with DAPI (*blue*). *Bar*, 10 μm.

ifies nuclear location (17, 18, 20, 21, 23, 24). To clarify structure-function relationship, we constructed several hsSUN1 deletion mutants (Fig. 1*B*) and expressed each in HeLa cells. We observed that hsSUN1 despite removal of amino acids 480–785 (Fig. 1*C*, *panels 1–3*, see WT, ΔC1, and ΔC2 proteins) still retained a nuclear envelope pattern indicating that hsSUN1 C terminus, including its SUN domain, is dispensable for nuclear membrane localization. When we deleted into hsSUN1 coiled-coils, as in hsSUN1 ΔC3, ~10% of the protein partitioned from the nuclear envelope into the cytoplasm (Fig. 1*C*, *panel 4*). Further removal of all three transmembrane regions (amino acids 1–238, ΔC4; Fig. 1*C*, *panel 5*) dispersed increased amounts of hsSUN1.

The above analyses were complemented with deletions starting from the N terminus. Removing the first 102 N-terminal amino acids from hsSUN1 (amino acids 103–785 ΔN1, Fig. 1*C*, *panel 6*) shifted more than 60% of the protein from the envelope into the ER. Removing the next 102 amino acids (amino acids 205–785 ΔN2, Fig. 1*C*, *panel 7*) did not cause further changes. However, when the deletion was extended to amino acid 306, hsSUN1 ΔN3 (amino acids 307–785) became wholly cytoplasmic (Fig. 1*C*, *panel 8*). Collectively, the results show hsSUN1 three putative transmembrane motifs and its first 102 N-terminal amino acids are needed for retention in the nuclear envelope.

HsSUN1 Nucleates Daughter Nuclear Envelope Formation—Because antibodies are not available, we generated and affinity-purified rabbit antisera (αhsSUN1-C) to hsSUN1 C-terminal 362–785 amino acids (Fig. 2*A*). Using αhsSUN1-C, we first studied the distribution of cell endogenous hsSUN1. Interphase hsSUN1 stained with lamin B1 around the nucleus (Fig. 2*B*). In early mitosis even as the envelope commences breakdown, hsSUN1, along with lamin B1 and emerin, is found at the nuclear membrane, (Fig. 2*C*, *panels 1–6*). During this period, hsSUN1 and the nuclear pore complex (NPC, detected with mab414, which recognizes the conserved FXFG repeats in

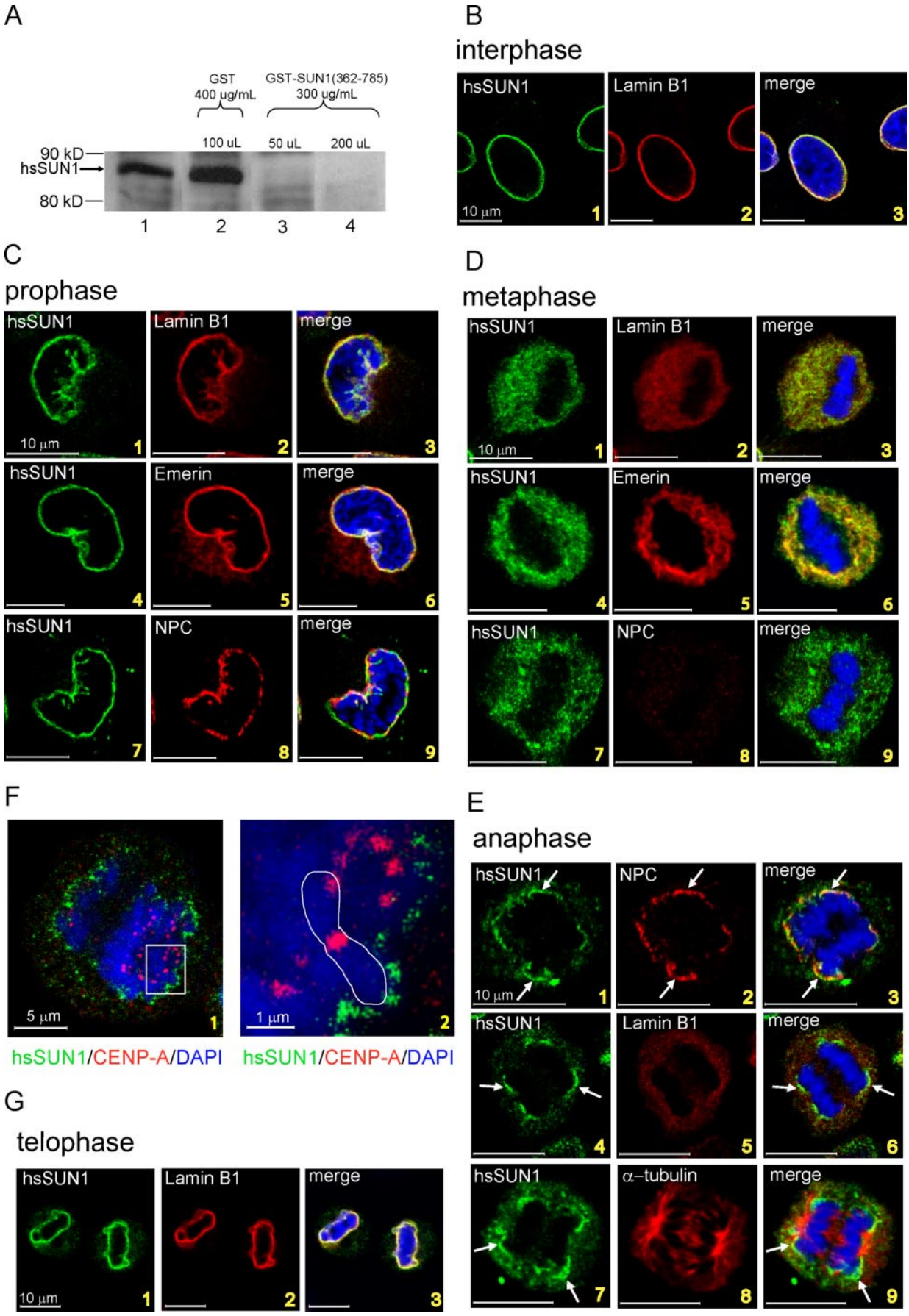

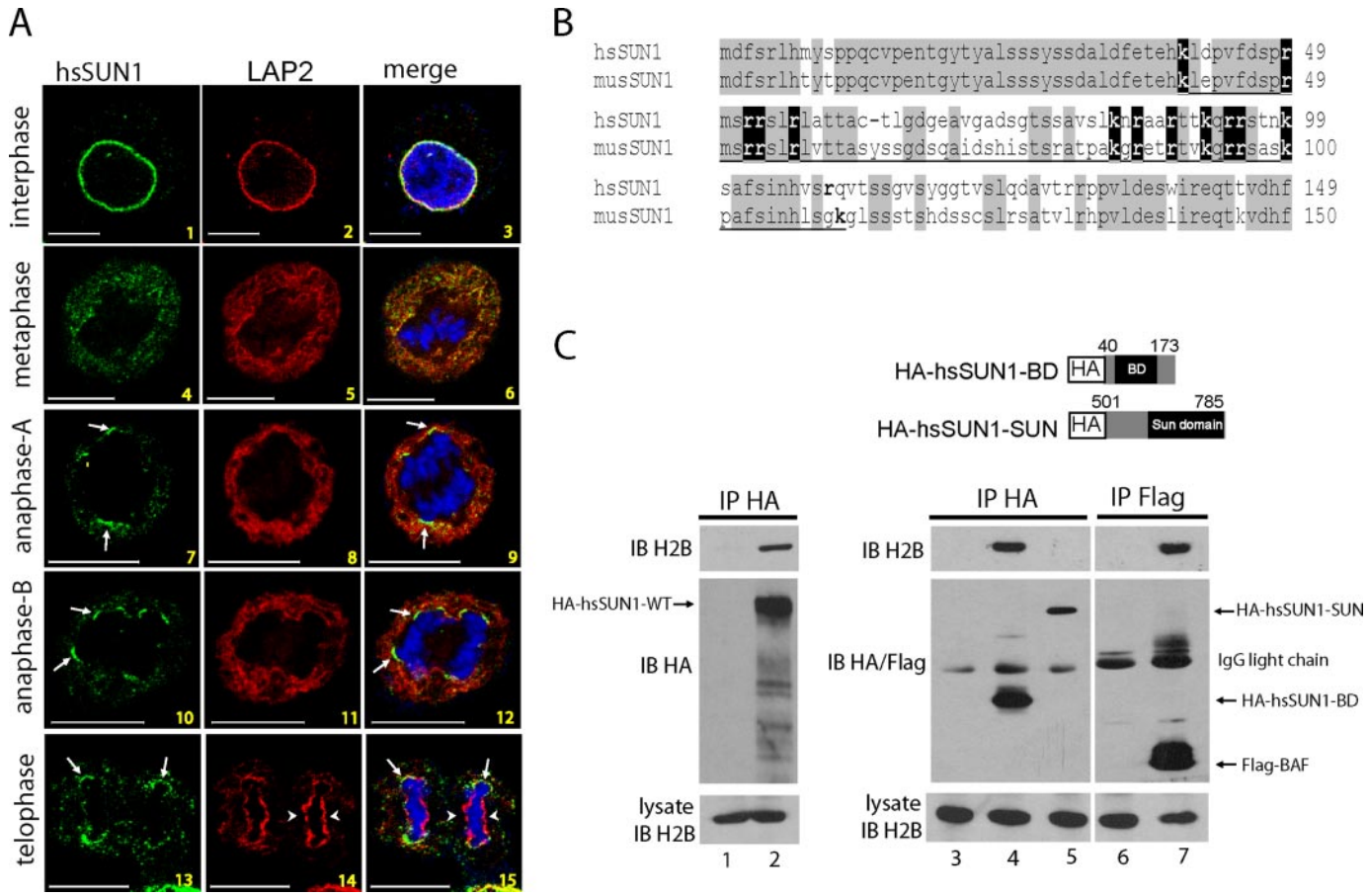

FIGURE 3. **HsSUN1 binds chromatin prior to LAP2.** *A*, localization of hsSUN1 (*green*) and LAP2 (*red*) were compared in interphase (*panels 1–3*), metaphase (*panels 4–6*), anaphase (*panels 7–12*), and telophase (*panels 13–15*) cells. HsSUN1 appears first at the peripheral rim of separated sister chromatids, as denoted by *arrows* with LAP2 appearing later (indicated by *arrowheads*). DNA was stained with DAPI (*blue*). *Bar*, 10 μm. *B*, alignment of N-terminal amino acids of human and mouse SUN1. Identities are shaded in *gray*; conserved basic amino acids are shaded in *black*. The basic domains of human and mouse SUN1 are *underlined*. *C*, chromatin binding assay was performed using HeLa cells expressing transfected full-length HA-hsSUN1-WT (*lane 2*), HA-hsSUN1-BD (*lane 4*), or HA-hsSUN1-SUN (*lane 5*), or FLAG-BAF (*lanes 7*). *Lanes 1*, *3*, and *4* are mock-transfected samples. Cell lysates were immunoprecipitated with monoclonal anti-HA- (*lanes 1–5*) or monoclonal anti-FLAG- (*lanes 6* and *7*) agarose beads. Histone H2B co-immunoprecipitated by HA-hsSUN1-BD or FLAG-BAF was detected by immunoblotting.

nucleoporins) are partially overlapping (Fig. 2*C*, *panels 7–9*). As the cell moves into metaphase, hsSUN1, lamin B1, and emerin disperse into the mitotic cytosol (Fig. 2*D*, *panels 1–6*) while NPC-staining with mab414 is extinguished (Fig. 2*D*, *panels 7–9*). By anaphase, hsSUN1 reorganizes around nascently separated daughter DNAs (Fig. 2*E*) at the peripheral edges of condensed chromosomes (see Fig. 2*F*; compare the locations of hsSUN1 and CENP-A). We note that as hsSUN1 reforms structurally from metaphase to anaphase NPC-staining follows coincidentally (Fig. 2*E*, *panels 1–3*). By contrast, re-organization of anaphase lamin B1 (Fig. 2*E*, *panels 4–6*) lags initially (compare NPC and lamin B1 staining relative to α-tubulin-staining; Fig. 2*E*, *panels 2*, *5*, and *8*); but by telophase, lamin B1 too converges with hsSUN1 at newly reformed daughter nuclear envelopes (Fig. 2*G*). While other interpretations are possible, these sequential views suggest that hsSUN1 leads NPC and lamin B1 in nucleating daughter envelopes.

HsSUN1 Congresses to Newly Segregated Chromosomes before LAP—Above, anaphase hsSUN1 precedes lamin B1 in reorganizing around newly segregated chromosomes (Fig. 2*E*). Previously, LAP2 and LBR were reported as INM proteins (25–27) with congruent timing in their association with partitioning mitotic chromosomes (25, 28–30). We next queried whether the hsSUN1 association with segregated chromatids (Fig. 2*E*) occurs prior to or after LAP2/LBR.

To assess the relative ordering of hsSUN1 and LAP2, we immunostained simultaneously cell-endogenous hsSUN1 and LAP2. HsSUN1 and LAP2 are together in interphase (Fig. 3*A*, *panels 1–3*). By metaphase, both hsSUN1 and LAP2 become dispersed (Fig. 3*A*, *panels 4–6*). In early anaphase, hsSUN1

FIGURE 2. **Cell cycle localization of hsSUN1.** *A*, characterization of the specificity of affinity-purified αhsSUN1-C in Western blotting experiments using competition with either an excess of GST (*lane 2*) or GST-hsSUN1-(362–785) proteins (*lanes 3* and *4*). *B–G*, fixed HeLa cells were immunostained with αhsSUN1-C (*green*) antibody and antibodies, as indicated, to lamin B1, emerin, NPC (mab414), α-tubulin, or CENP-A. Interphase *B*, prophase *C*, metaphase *D*, anaphase *E* and *F*, and telophase *G* cells are shown. DNA was stained with DAPI (*blue*). *F*, two views (*panels 1* and *2*) of anaphase cells stained with hsSUN1 (*green*) and CENP-A (*red*). *Panel 2* shows an enlarged view of hsSUN1 at the edge of segregated chromosomes in anaphase. *Arrows* in *E* point to hsSUN1 at the lateral margins of anaphase chromosomes.

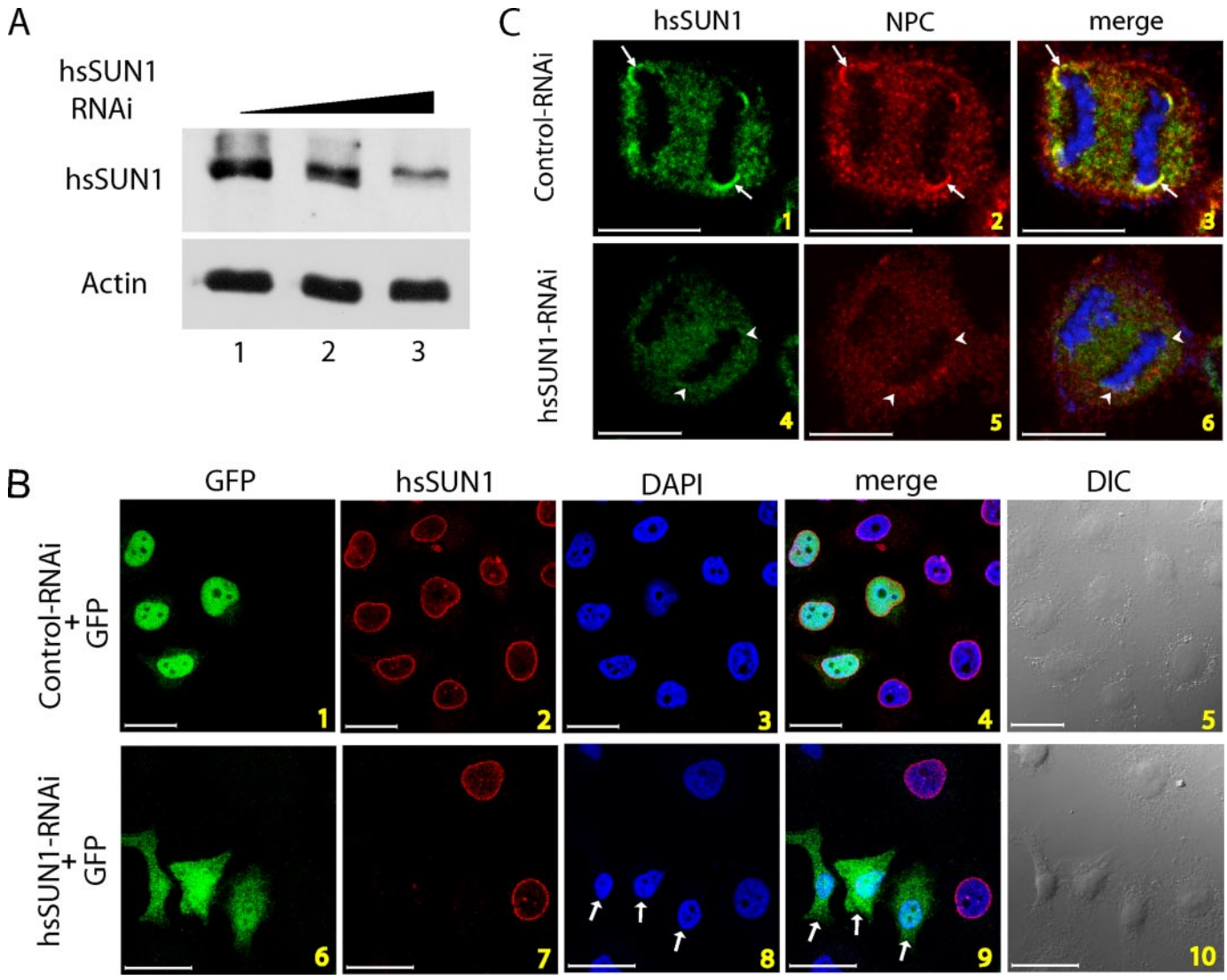

FIGURE 4. **Depletion of hsSUN1 impairs nuclear envelope integrity and NPC formation.** *A*, immunoblotting of lysates from cells treated with 0, 1, or 4 μg (*lanes 1–3*) of hsSUN1 siRNA and probed with αhsSUN1-C. Actin was used as a loading control. *B*, HeLa cells were co-transfected with a GFP-expressing plasmid and control- (*panels 1–5*) or hsSUN1- (*panels 6–10*) siRNA and immunostained with αhsSUN1-C. GFP is *green*; hsSUN1 is *red*; and DNA (DAPI) is *blue*. GFP-expressing cells (*arrows*) indicate cells transfected with siRNA. *Bar*, 10 μm. *C*, control- (*panels 1–3*) or hsSUN1- (*panels 4–6*) siRNA transfected cells were stained using αhsSUN1-C (*green*, *panels 1* and *4*) and mab414 (NPC, *red*, *panels 2* and *5*). DAPI (*blue*) was used to visualize DNA. *Bar*, 10 μm.

reorganizes at the peripheral edges of chromosomes (Fig. 3*A*, *panels 7–9*) with LAP2 following later to chromosome proximal locales (Fig. 3*A*, *panels 10–15* and Ref. (27)). These comparisons place hsSUN1 interaction with newly segregated chromosomes before LAP2.

A current notion is that LAP2/LBR forms a scaffold onto which other NE proteins coalesce to assemble a new nuclear envelope. LAP2 and LBR contain basic amino acid chromatin-binding domains (31). Because SUN1 associates with segregated chromosomes before LAP2, we wondered if SUN1 also has a chromatin-binding domain. We compared human and mouse SUN1 sequences and noted that both conserved a basic N-terminal amino acid region (hsSUN1 amino acids 40–109; musSUN1 amino acids 40–111; both pIs are 11.5, Fig. 3*B*). To check if this N-terminal fragment can bind chromatin, we overexpressed HA-tagged wild type full-length hsSUN1 (hsSUN1-WT) and the hsSUN1 basic domain (hsSUN1-BD, amino acids 40–173, Fig. 3*C*) and performed a modified chromatin precipitation assay (as described under "Experimental Procedures"). As a positive control, the known chromatin-binding protein, BAF (barrier-to-autointegration factor), was used in a parallel assay (Fig. 3*C*, *lane 7*). Indeed, full-length hsSUN1-WT and hsSUN1-BD co-precipitated histone H2B (Fig. 3*C*, *lanes 2* and *4*) like BAF (Fig. 3*C*, *lane 7*); by contrast, a protein containing only the hsSUN1 SUN domain (hsSUN1-SUN, amino acids 501–785) did not (Fig. 3*C*, *lane 5*). These results identify a chromatin-association domain in the N terminus of hsSUN1.

Cells Depleted for hsSUN1 Have Defective Nuclear Envelope—Next, using RNAi-mediated depletion, we characterized the requirement for hsSUN1 in nuclear envelope integrity (Fig. 4*A*). HsSUN1-siRNA or control-siRNAi was introduced separately into cells with a nuclear-targeted green fluorescent protein (GFP). Green cells from hsSUN1-siRNA or control-siRNA transfections were compared, and hsSUN1 protein was found to be depleted from the former but not the latter (Fig. 4*B*, compare *panel 7* to *panel 2*). Interestingly, whereas nuclear-tar-

geted GFP was wholly circumscribed in the nucleus in control-RNAi cells (compare GFP to DAPI, Fig. 4*B*, *panels 1* and *3*), the GFP protein showed a whole-cell distribution in hsSUN1-RNAi cells (Fig. 4*B*, *panels 6* and *8*). This latter profile suggests a nuclear envelope defect in hsSUN1-depleted cells, which fail to retain nuclear-targeted GFP.

To independently check nuclear envelope integrity, we stained for NPC. In control cells, NPC staining was seen appropriately in anaphase (Fig. 4*C*, *panels 1–3*; Refs. 32, 33). By contrast, hsSUN1-RNAi cells were absent for hsSUN1 and showed failed NPC staining/reorganization at the edges of segregated DNA masses in anaphase (Fig. 4*C*, *panels 4–6*, *arrowheads*). Hence, hsSUN1 appears to be required in anaphase for NPC formation; failed NPC assembly may explain the inability of nuclear envelope to retain nuclear-GFP (Fig. 4*B*, *panels 6* and *9*).

hsSUN1-depleted Cells Have Delayed Chromosome De-condensation—Two events occur at the end of mitosis: daughter nuclei form and chromosomes de-condense. Currently, it is unclear whether these two events are linked. To ask if the daughter nuclear envelope reassembly influences DNA de-condensation, we visualized chromosome segregation in control and hsSUN1 RNAi cells. We digitized signals from DAPI-stained chromosomes using heightened colored intensities to reflect increased DNA compaction (Fig. 5*A*, *panels 4* and *8*). By this measure, control-RNAi cells compared with hsSUN1-RNAi cells at the same juncture during cell division (as monitored by α-tubulin staining) had consistently lower DAPI intensity (see Fig. 5*A*, *panels 4* and *8*; the averaged fluorescent intensity is 2.7 times lower in *panel 4* than *panel 8*). Thus, hsSUN1 depletion affects nuclear envelope integrity (Fig. 4*B*) and results in an apparent increase in DNA compaction (Fig. 5*A*).

An apparent enhancement in DNA compaction could arise from a relative delay in de-condensation of condensed chromosomes. We next captured time lapse images in live cells transfected with hsSUN1-siRNA or control siRNA and a green fluorescent histone H2B (GFP-H2B) plasmid. GFP-H2B expression in live cells permits the dynamic visualization of fluorescent mitotic chromatin. In timed comparisons, chromosomes de-condensed 24–36 min after commencing anaphase-imaging in control siRNA cells (Fig. 5*B*, *panels 1–12*), but chromosomes remained condensed even after 60 min (Fig. 5*B*, *panels 13–24*) in hsSUN1 siRNA cells. We replicated 22 pairs of time lapse experiments. In total, 32% (7 of 22) of hsSUN1-RNAi cells showed marked delayed in de-condensation, and 42% (3 of 7) of these "delayed" cells failed to complete mitosis and succumbed to apoptosis; on the other hand, all 22 control time lapses proceeded through mitosis with normal kinetics (Fig. 5*B* and data not shown).

Acetylation of Histone H2B and H4 Is Decreased in hsSUN1-depleted Cells—We sought to understand what accounted for delayed chromosome de-condensation in hsSUN siRNA cells. Condensed chromosomes are wrapped by histones whose function is regulated by post-translational acetylation and phosphorylation among other events (34–36). Phosphorylation of histone H3 at serine 10 (H3pSer10) was previously proposed to initiate chromatin condensation when cells enter mitosis (37). On the other hand, what event specifies chromatin de-condensation as cells exit mitosis is unknown. In our experiments, H3pSer10 phosphorylation in anaphase and telophase did not differ between hsSUN1 and control RNAi cells (supplemental Fig. S1), suggesting that this event does not explain results in Fig. 5*B*.

Histone acetylation modulates compacted chromatin to allow transcription factors to access DNA (38, 39). We wondered whether histone acetylation might also regulate mitotic DNA de-condensation. To investigate this notion, the acetylation status of histones in control and hsSUN1 RNAi cells was characterized by Western blotting (Fig. 5*C*). Total acetylated H2B (AcH2B; Fig. 5*C*), determined using a mixture of antibodies individually specific for acetyl-Lys^{5}, -Lys^{12}, -Lys^{15}, and -Lys^{20}, and acetylated H4 (AcH4; Fig. 5*C*), verified with an antibody mix specific for acetyl-Lys^{5}, -Lys^{8}, -Lys^{12}, and -Lys^{16}, were reduced in hsSUN1-RNAi *versus* control RNAi samples. On the other hand, acetylated H3 (AcH3; Fig. 5*C*) was insignificantly changed. We next analyzed several individual lysine acetylation sites in H2B and H4. HsSUN1-RNAi cells were significantly reduced for acetylation at Lys^{12} and Lys^{15}, but not at Lys^{5}, of H2B; and for acetylation at Lys^{8}, Lys^{12}, and Lys^{16} of H4 (Fig. 5*D*). These results show that depletion of hsSUN1 not only affected nuclear envelope integrity (Fig. 4) and mitotic chromosome de-condensation (Fig. 5, *A* and *B*), but also the acetylation of H2B and H4 (Fig. 5, *C* and *D*).

hALP Contributes to Chromosome De-condensation—The above results suggest that mitotic chromosome de-condensation is linked to a histone acetyltransferase (HAT) activity. To ask which HAT contributes this activity, we reasoned that such a HAT must be a nuclear membrane-associated moiety. An *in silico* search revealed that the human genome encodes a minimum of sixteen HATs (40, 41); however, only one, KIAA1709/hALP (41), is a nuclear membrane-associated protein (5).

We investigated whether hALP would interact with mitotic DNA. In mitotic cells, hALP was stained with condensed chromosome in a sheath-like array (Fig. 6*A*; Ref. 42). Such interaction is compatible with hALP providing a HAT activity for de-condensing mitotic chromosomes. Indeed, consistent with this interpretation, when we used siRNA to deplete hALP (Fig. 6, *B* and *C*) and followed in time lapse GFP-H2B-marked DNA de-condensation, prolonged chromosome condensation was seen in hALP-siRNA cells compared with control cells (Fig. 6*D*).

hsSUN1 Targets hALP Activity to Chromosomes—A plausible model from our results is that condensed mitotic chromosomes as they become wrapped by newly forming daughter nuclear envelope contact the chromatin-binding domain of hsSUN1, which brings membrane-associated hALP to facilitate DNA de-condensation. This model which suggests that hsSUN1 targets hALP to condensed chromosome can be tested by constructing a chimeric protein with the chromatin binding domain of hsSUN1 (Fig. 3*B*) fused to hALP. A prediction is that an N terminus hsSUN-hALP fusion would directly target chromatin and would enhance DNA de-condensation.

We thus constructed an in-frame fusion of an N-terminal portion of hsSUN1, hsSUN1ΔC4 (amino acids 1–238), with

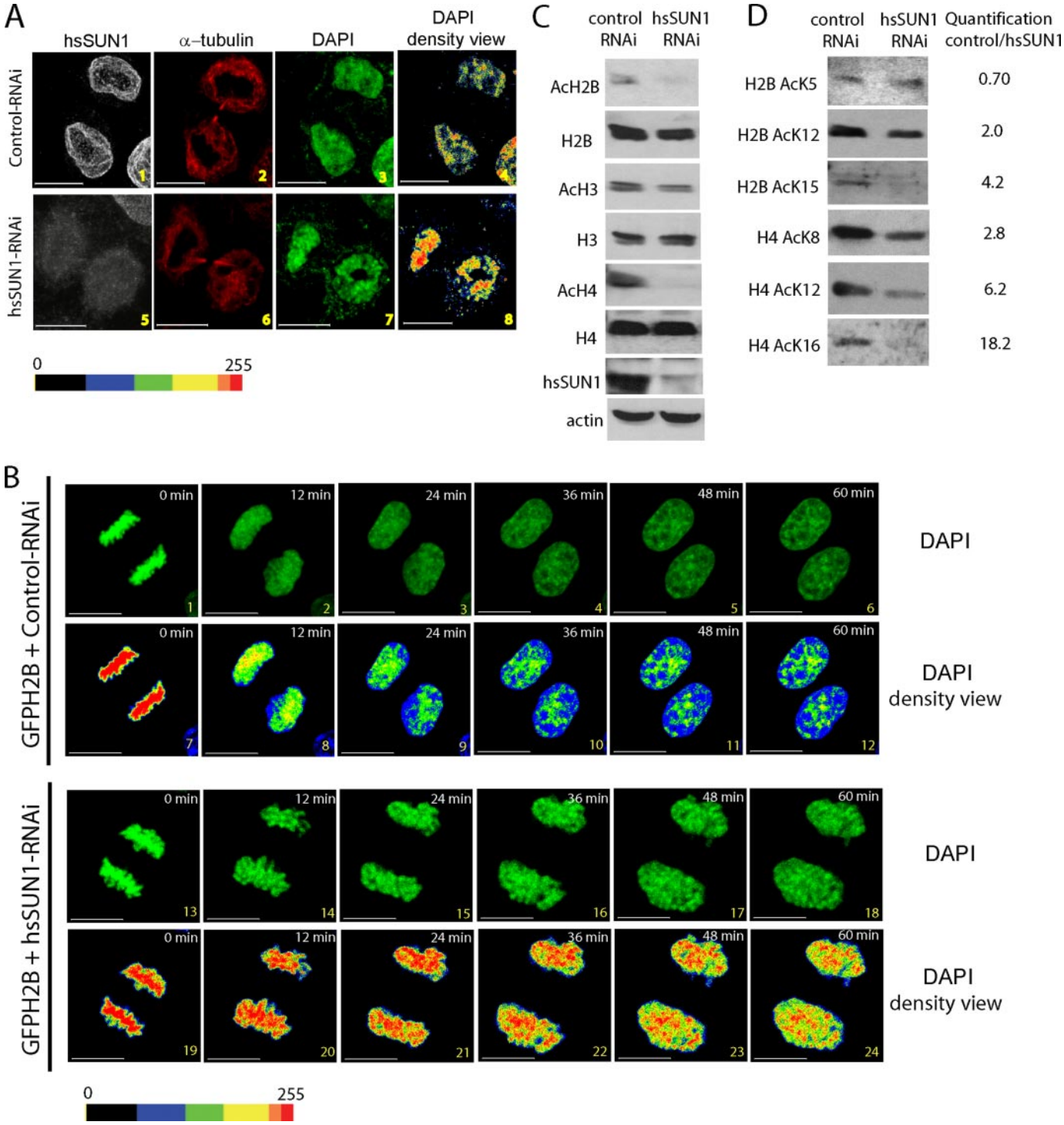

FIGURE 5. **Knockdown of hsSUN1 prolonged chromatin condensation with hypoacetylated histones.** *A*, cells transfected with control- or hsSUN1-siRNA were immunostained to visualize hsSUN1 (*gray*, *panels 1* and *5*) and α-tubulin (*red*, *panels 2* and *6*). DNA was stained with DAPI (*green*, *panels 3* and *7*). In *panels 4* and *8*, intensities of DNA staining were digitized in 256 bits and color coded by a range of colors (from high to low: *red*, *orange*, *yellow*, *green*, *blue*, and *black*) as presented at the *bottom*. Sum of z-stack images are shown. *Bar*, 10 μm. *B*, time-lapse imaging of GFP-H2B in live cells transfected with control- (*panels 1–12*) or hsSUN1-siRNA (*panels 13–24*). Sum of z-stack images are presented. Fluorescent intensities of GFP-H2B (*top*, *panels 1–6* and *13–18*) were digitized and color coded (*bottom*, *panels 7–12* and *19–24*) as in *A*. *Bar*, 10 μm. *C*, cellular extracts from cells transfected with control- or hsSUN1-siRNA were analyzed by Western blotting using a mixture of antibodies against individually acetylated lysines in histone H2B (*K5*, *K12*, *K15*, or *K20*), histone H3 (*K9*, *K14*), or histone H4 (*K5*, *K8*, *K12*, *K16*). *D*, cellular extracts described in *C* were analyzed by Western blotting using a mixture of antibodies individually targeted to the indicated acetyl-lysine. Acetylations were quantified by densitometry (ImageJ software version 1.34S, NIH) and scored at *right*.

hALP creating hsSUN1ΔC4-hALP (Fig. 7*A*). HsSUN1ΔC4 contains the hsSUN1 chromatin binding domain and its inner membrane-associated domain. We then separately transfected hsSUN1ΔC4-hALP, hsSUN1ΔC4, or hALP with GFP-H2B into cells. For each of the three transfection groups, we studied 20 mitotic nuclei using time-lapse imaging. In hsSUN1ΔC4 cells, one out of twenty nuclei showed earlier than normal de-condensation; in hALP cells, zero out of twenty showed

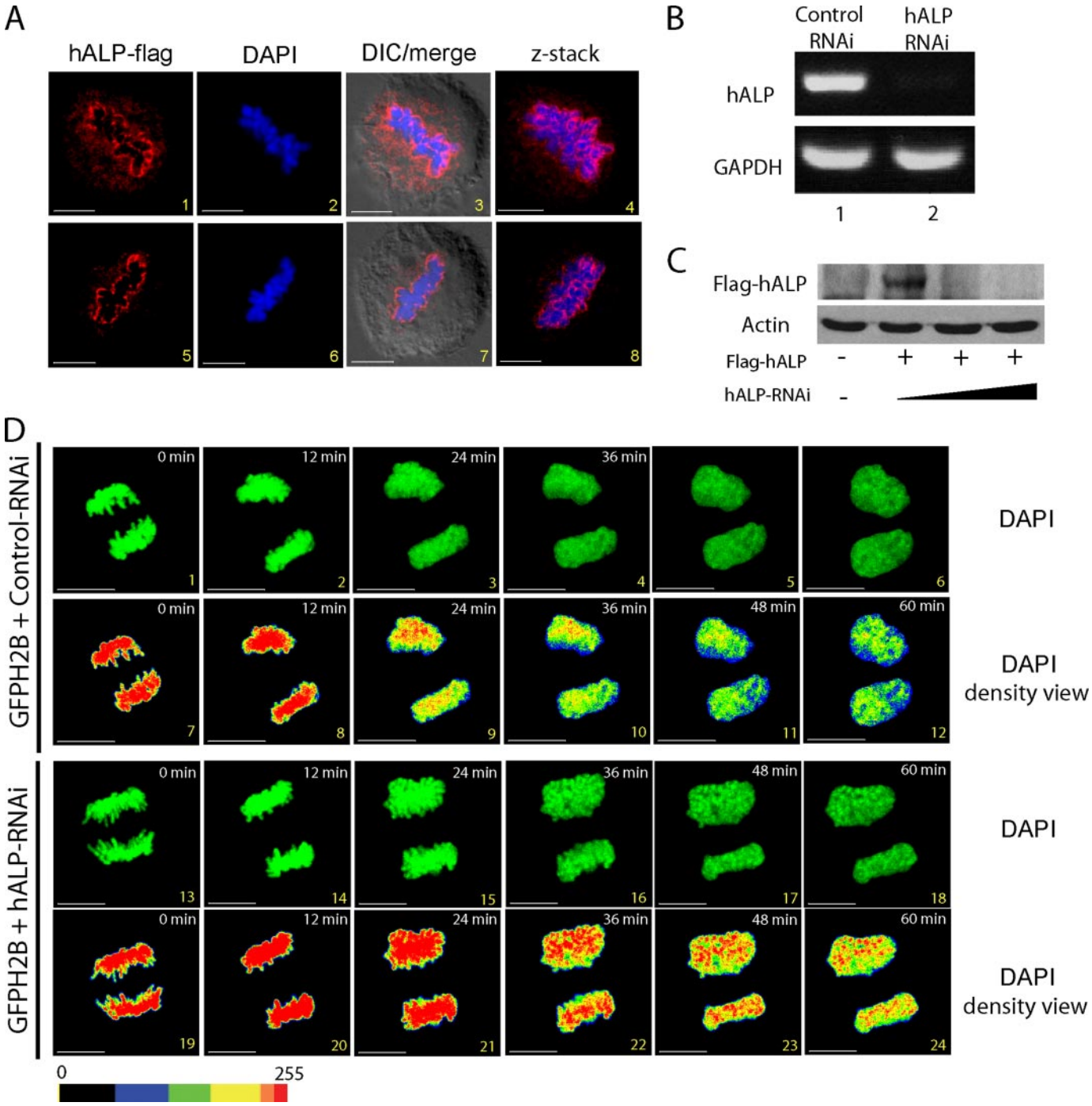

FIGURE 6. **Depletion of hALP prolonged DNA condensation.** *A*, localization of hALP with DNA. Cells transfected with hALP-FLAG was immunostained with anti-FLAG (*red*). DNA stained with DAPI is in *blue*. Images of hALP and DAPI staining were merged with light field views (*DIC*). *Bar*, 10 μm. *B*, expression of endogenous hALP mRNA in control-siRNA (*lane 1*) and hALP-siRNA (*lane 2*) transfected cells was assessed by RT-PCR. GAPDH RNA was used as control. *C*, Western blotting verification of knockdown of hALP-FLAG protein by hALP-siRNA. Protein loadings were normalized to actin. *D*, time-lapse images of GFP-H2B in live cells transfected with hALP-siRNA (*left*) or control-siRNA (*right*). Sum of z-stack images are presented. Fluorescent intensities of GFP-H2B were digitized and color-coded (*panels 7–12* and *19–24*) as in Fig. 5. *Bar*, 10 μm.

kinetics of de-condensation different from mock-transfected controls (Fig. 7*B* and supplemental movie 1A). By contrast, 30% (six of twenty) of hsSUN1ΔC4-hALP cells underwent premature DNA de-condensation, even before clear separation of sister chromatids occurred (Fig. 7*B* and supplemental movie 1B).

The findings from the artificial hsSUN1ΔC4-hALP fusion protein are consistent with hsSUN1 bridging hALP interaction with DNA. To ask if an intracellular bridging interaction could be explained by protein-protein binding between hsSUN1 and hALP, we assayed whether overexpressed hsSUN1ΔC4A co-immunoprecipitates hALP. As a control, we also used a deleted version of hsSUN1, which contains only its SUN domain (*i.e.* hsSUN1-SUN, Fig. 3*C*). Cell lysates from respectively transfected cells were prepared and co-immunoprecipitations were performed. Fig. 7*C* shows that hALP indeed co-precipitated

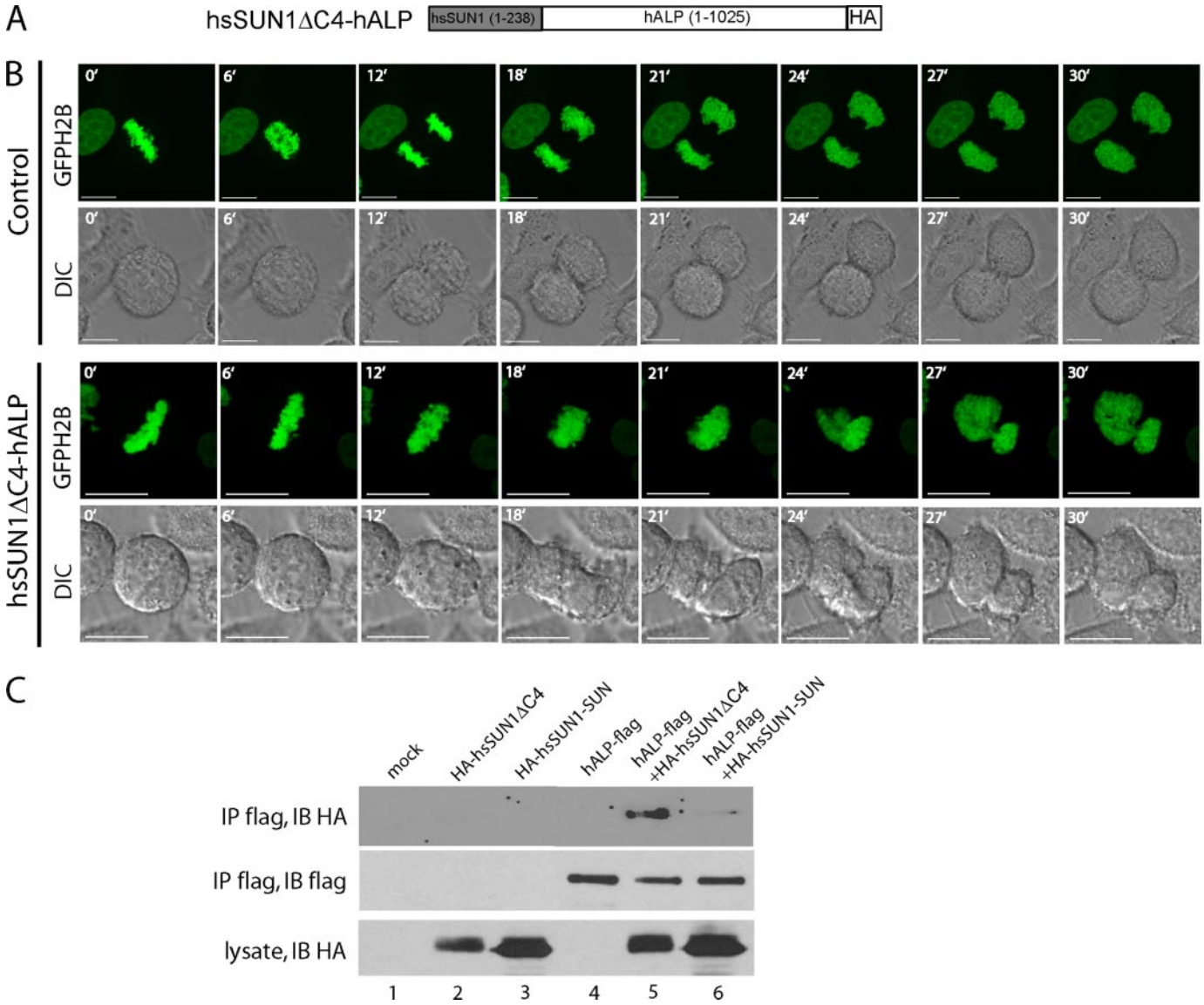

FIGURE 7. **hSUN1 and hALP function in mitotic chromosome de-condensation.** *A*, schematic representation of hsSUN1ΔC4-hALP fusion protein. *B*, GFP-H2B (*green*) and light field (*DIC*) time-lapse images of cells transfected with control or hsSUN1ΔC4-hALP plasmids. Sum of z-stack images are presented. *Bar*, 10 μm. *C*, hALP-FLAG was immunoprecipitated from cell extracts coexpressing HA-tagged hsSUN1ΔC4 (*lane 5*) or hsSUN1-SUN (*lane 6*). hALP-FLAG and co-immunoprecipitating hsSUN1ΔC4 (*lane 5*) were detected by immunoblotting.

with hsSUN1ΔC4 (Fig. 7*C*, *lane 5*) but not hsSUN1-SUN (Fig. 7*C*, *lane 6*).

DISCUSSION

Except for a shared SUN motif, hsSUN1 is unrelated in sequence to other SUN proteins. HsSUN1 has three predicted transmembrane domains. Here, we show that the hsSUN1 three transmembrane domains are needed for nuclear membrane retention and that its N terminus is needed for chromatin binding. Additional evidence shows that hsSUN1 serves an early role in the proper reformation of daughter nuclear envelopes and in targeting hALP to chromosomes.

Chromosomes are structurally organized and occupy discrete nuclear territories (43). The nuclear envelope provides a scaffold for anchoring chromatin and for maintaining nuclear integrity (32, 44). Nuclear envelope and associated proteins such as nuclear lamina, NPC, LAP2, LBR, and emerin directly or indirectly interact with chromatin to regulate DNA replication and transcription (27, 43, 45). A pivotal event in the mammalian cell cycle is nuclear membrane dissolution as a cell enters mitosis. Much about nuclear envelope breakdown and reassembly remain incompletely understood (33, 46–48). Recent findings suggest that nuclear envelope proteins first reassembles via tethering to discrete regions on segregated chromatids (27, 29, 30, 49, 50). Which protein sets the stage for others to follow has not been fully defined. Here, we report that hsSUN1 precedes LAP2 and lamin B1 in interacting with segregated chromosomes in anaphase. Whether hsSUN1 is the first INM or follows a yet earlier protein is unclear. However, findings that hsSUN1 has a chromatin binding domain in its N terminus and that its depletion leads to failed NPC formation

(Fig. 4*C*) and delayed chromosome de-condensation (Fig. 5*B*) position this protein as an important non-redundant critical player at the end of mitosis.

Mitotic chromosomes are thought to be highly compacted for physical reasons required for segregation. After separating sister chromatids, the completion of mitosis mandates that new envelopes reform around DNA to consummate two daughter nuclei. Transcription is silenced in mitosis as expected for highly condensed chromatin (51). However, the start of the next cell cycle (*i.e.* G1) needs *de novo* mRNA synthesis from de-condensed genes (52, 53). While it is accepted that as a cell begins mitosis DNA condensation correlates with phosphorylation of Ser^{10} on H3 (37), what dictates DNA de-condensation at the end of mitosis is less clear. Our data now suggest that the signal to trigger de-condensation is not a change at phosphorylated H3Ser10 (supplemental Fig. S1). Instead, our findings indicate that de-condensation is marked by several acetylated lysines in H2B and H4 (Fig. 5, *C* and *D*), including Lys^{15} of H2B and Lys^{8}, Lys^{12}, and Lys^{16} of H4. Acetylation of specific lysine(s) in histones has been extensively reported to regulate transcriptional activation, histone deposition, DNA repair, and chromatin structure (35, 54). Increasing evidence has led to the idea of a histone modification code, which might be recognized by various cellular machineries. We suggest hsSUN1 is responsible for inducing the acetylation a subset of histones at the end of mitosis and generating a code for the initiation of chromosome de-condensation. An unexpected result from our work is that chromosome segregation does not appear to be obligatory for DNA de-condensation. Hence, a chromatin-targeted HAT is sufficient to initiate DNA de-condensation of duplicated sister chromatids that have yet to separate fully (Fig. 7*B*, see supplemental movie 1).

Our results suggest three ways to view the link between hsSUN1 and chromatin de-condensation/histone acetylation. The first view is that hsSUN1 modulates histone acetyltransferases (HATs), or histone deacetylases (HDACs), which modifies H2B and H4. Perturbation of this HAT (HDAC)-activity leads to (de)acetylated H2B and H4 (Fig. 5*C*), which promotes chromatin (de)compaction. A second view is that DNA de-condensation requires the proper completion of a daughter nuclear envelope. Here, loss of hsSUN1 interrupts nuclear membrane reassembly thereby interfering with de-condensation. That defects in BAF (55) and nuclear lamina (56) also affect nuclear envelope formation and retard chromatin de-condensation are consistent with this latter perspective. A third view is that both of the above two processes are important. Accordingly, in the context of a reforming daughter envelope an INM protein is used to recruit a HAT (HDAC) for purposes of regulating DNA de-condensation. Indeed, reports that LAP2β can interact with HDAC3 and contribute to histone H4 deacetylation (57) are compatible with a mechanistic model in which interplay between HATs and HDACs at the termination of mitosis tips the DNA condensation/de-condensation balance.

If a HAT is needed, then which HAT works with hsSUN1? While many HATs exist in the human genome, only one, hALP, based on proteomic data (5), is nuclear membrane-associated. Moreover, hALP was detected in mitotic chromosome scaffold fraction by proteomics, supporting its role in mitosis (42). Three pieces of evidence support the relevance of hALP for chromosome de-condensation: 1) hALP congresses to mitotic DNA (Fig. 6*A*); 2) knockdown of hALP prolongs DNA condensation (Fig. 6*D*); and 3) direct targeting of hsSUN1ΔC4-hALP to chromatin accelerates DNA de-condensation (Fig. 7*B*). Hence, while we cannot exclude the involvement of other HATs and/or HDACs, our results are consistent with requirements for hALP and hsSUN1 in mitotic DNA de-condensation. What remains possible is that hsSUN1 may interact with other nuclear or nuclear matrix-associated HATs in addition to nuclear-membrane associated hALP. Such additional interactions, if identified, could also contribute to mitotic DNA de-condensation. Indeed, understanding how condensed mitotic chromatin is de-condensed complements insights on how heterochromatin is transformed into a transcriptionally active state (58). These complementary studies add to the richness of our appreciation for the regulatory roles played by histones in chromosome biology (59).

Acknowledgments—We thank Kazusa DNA Research Institute, Japan for providing cDNA encoding hsSUN1 and hALP; Dr. Manfred Wehnert at Institute of Human Genetics, Germany for providing lymphoblastoid cell lines; Drs. V. Yedavalli, H. Iha, Y. Bennasser, B. Lafont for experimental discussions and Y. Li for technical assistance; and John Hanover and members of the Jeang laboratory for critical reading of the manuscript.

REFERENCES

1. Taddei, A., Hediger, F., Neumann, F. R., and Gasser, S. M. (2004) *Annu. Rev. Genet.* **38,** 305–345
2. Fahrenkrog, B., Koser, J., and Aebi, U. (2004) *Trends Biochem. Sci.* **29,** 175–182
3. Hutchison, C. J. (2002) *Nat. Rev. Mol. Cell. Biol.* **3,** 848–858
4. Mattout-Drubezki, A., and Gruenbaum, Y. (2003) *Cell Mol. Life Sci.* **60,** 2053–2063
5. Schirmer, E. C., Florens, L., Guan, T., Yates, J. R., III, and Gerace, L. (2003) *Science* **301,** 1380–1382
6. Burke, B. (2001) *Nat. Cell Biol.* **3,** E273–E274
7. Burke, B., Mounkes, L. C., and Stewart, C. L. (2001) *Traffic* **2,** 675–683
8. Burke, B., and Stewart, C. L. (2002) *Nat. Rev. Mol. Cell. Biol.* **3,** 575–585
9. Worman, H. J., and Courvalin, J. C. (2004) *J. Clin. Investig.* **113,** 349–351
10. Holaska, J. M., Wilson, K. L., and Mansharamani, M. (2002) *Curr. Opin. Cell Biol.* **14,** 357–364
11. Holmer, L., and Worman, H. J. (2001) *Cell Mol. Life Sci.* **58,** 1741–1747
12. Shumaker, D. K., Kuczmarski, E. R., and Goldman, R. D. (2003) *Curr. Opin. Cell Biol.* **15,** 358–366
13. Starr, D. A., and Han, M. (2003) *J. Cell Sci.* **116,** 211–216
14. Malone, C. J., Fixsen, W. D., Horvitz, H. R., and Han, M. (1999) *Development* **126,** 3171–3181
15. Hagan, I., and Yanagida, M. (1995) *J. Cell Biol.* **129,** 1033–1047
16. Lee, K. K., Starr, D., Cohen, M., Liu, J., Han, M., Wilson, K. L., and Gruenbaum, Y. (2002) *Mol. Biol. Cell* **13,** 892–901
17. Crisp, M., Liu, Q., Roux, K., Rattner, J. B., Shanahan, C., Burke, B., Stahl, P. D., and Hodzic, D. (2006) *J. Cell Biol.* **172,** 41–53
18. Padmakumar, V. C., Libotte, T., Lu, W., Zaim, H., Abraham, S., Noegel, A. A., Gotzmann, J., Foisner, R., and Karakesisoglou, I. (2005) *J. Cell Sci.* **118,** 3419–3430
19. Dreger, M., Bengtsson, L., Schoneberg, T., Otto, H., and Hucho, F. (2001) *Proc. Natl. Acad. Sci. U. S. A.* **98,** 11943–11948
20. Hasan, S., Guttinger, S., Muhlhausser, P., Anderegg, F., Burgler, S., and Kutay, U. (2006) *FEBS Lett.* **580,** 1263–1268
21. Hodzic, D. M., Yeater, D. B., Bengtsson, L., Otto, H., and Stahl, P. D. (2004) *J. Biol. Chem.* **279,** 25805–25812

22. Kikuno, R., Nagase, T., Waki, M., and Ohara, O. (2002) *Nucleic Acids Res.* **30,** 166–168
23. Haque, F., Lloyd, D. J., Smallwood, D. T., Dent, C. L., Shanahan, C. M., Fry, A. M., Trembath, R. C., and Shackleton, S. (2006) *Mol. Cell. Biol.* **26,** 3738–3751
24. Wang, Q., Du, X., Cai, Z., and Greene, M. I. (2006) *DNA Cell Biol.* **25,** 554–562
25. Chaudhary, N., and Courvalin, J. C. (1993) *J. Cell Biol.* **122,** 295–306
26. Haraguchi, T., Koujin, T., Hayakawa, T., Kaneda, T., Tsutsumi, C., Imamoto, N., Akazawa, C., Sukegawa, J., Yoneda, Y., and Hiraoka, Y. (2000) *J. Cell Sci.* **113,** 779–794
27. Dechat, T., Gajewski, A., Korbei, B., Gerlich, D., Daigle, N., Haraguchi, T., Furukawa, K., Ellenberg, J., and Foisner, R. (2004) *J. Cell Sci.* **117,** 6117–6128
28. Buendia, B., and Courvalin, J. C. (1997) *Exp. Cell Res.* **230,** 133–144
29. Ellenberg, J., Siggia, E. D., Moreira, J. E., Smith, C. L., Presley, J. F., Worman, H. J., and Lippincott-Schwartz, J. (1997) *J. Cell Biol.* **138,** 1193–1206
30. Yang, L., Guan, T., and Gerace, L. (1997) *J. Cell Biol.* **137,** 1199–1210
31. Ulbert, S., Platani, M., Boue, S., and Mattaj, I. W. (2006) *J. Cell Biol.* **173,** 469–476
32. Hetzer, M. W., Walther, T. C., and Mattaj, I. W. (2005) *Annu. Rev. Cell Dev. Biol.* **21,** 347–380
33. Margalit, A., Vlcek, S., Gruenbaum, Y., and Foisner, R. (2005) *J. Cell. Biochem.* **95,** 454–465
34. de, l. C. X., Lois, S., Sanchez-Molina, S., and Martinez-Balbas, M. A. (2005) *Bioessays* **27,** 164–175
35. Shogren-Knaak, M., Ishii, H., Sun, J. M., Pazin, M. J., Davie, J. R., and Peterson, C. L. (2006) *Science* **311,** 844–847
36. Hake, S. B., Xiao, A., and Allis, C. D. (2004) *Br. J. Cancer* **90,** 761–769
37. Prigent, C., and Dimitrov, S. (2003) *J. Cell Sci.* **116,** 3677–3685
38. Narlikar, G. J., Fan, H. Y., and Kingston, R. E. (2002) *Cell* **108,** 475–487
39. Cheung, W. L., Briggs, S. D., and Allis, C. D. (2000) *Curr. Opin. Cell Biol.* **12,** 326–333
40. Gray, S. G., and Teh, B. T. (2001) *Curr. Mol. Med* **1,** 401–429
41. Lv, J., Liu, H., Wang, Q., Tang, Z., Hou, L., and Zhang, B. (2003) *Biochem. Biophys. Res. Commun.* **311,** 506–513
42. Gassmann, R., Henzing, A. J., and Earnshaw, W. C. (2005) *Chromosoma* **113,** 385–397
43. Marshall, W. F. (2002) *Curr. Biol.* **12,** R185–R192
44. Goldman, R. D., Gruenbaum, Y., Moir, R. D., Shumaker, D. K., and Spann, T. P. (2002) *Genes Dev.* **16,** 533–547
45. Somech, R., Shaklai, S., Amariglio, N., Rechavi, G., and Simon, A. J. (2005) *Pediatr. Res.* **57,** 8R–15R
46. Beaudouin, J., Gerlich, D., Daigle, N., Eils, R., and Ellenberg, J. (2002) *Cell* **108,** 83–96
47. Gant, T. M., and Wilson, K. L. (1997) *Annu. Rev. Cell Dev. Biol.* **13,** 669–695
48. Mattaj, I. W. (2004) *Nat Rev. Mol. Cell. Biol.* **5,** 65–69
49. Buendia, B., Courvalin, J. C., and Collas, P. (2001) *Cell Mol Life Sci* **58,** 1781–1789
50. Moir, R. D., Yoon, M., Khuon, S., and Goldman, R. D. (2000) *J. Cell Biol.* **151,** 1155–1168
51. Kruhlak, M. J., Hendzel, M. J., Fischle, W., Bertos, N. R., Hameed, S., Yang, X. J., Verdin, E., and Bazett-Jones, D. P. (2001) *J. Biol. Chem.* **276,** 38307–38319
52. Tumbar, T., Sudlow, G., and Belmont, A. S. (1999) *J. Cell Biol.* **145,** 1341–1354
53. Prasanth, K. V., Sacco-Bubulya, P. A., Prasanth, S. G., and Spector, D. L. (2003) *Mol. Biol. Cell* **14,** 1043–1057
54. Sterner, D. E., and Berger, S. L. (2000) *Microbiol. Mol. Biol. Rev.* **64,** 435–459
55. Segura-Totten, M., Kowalski, A. K., Craigie, R., and Wilson, K. L. (2002) *J. Cell Biol.* **158,** 475–485
56. Lopez-Soler, R. I., Moir, R. D., Spann, T. P., Stick, R., and Goldman, R. D. (2001) *J. Cell Biol.* **154,** 61–70
57. Somech, R., Shaklai, S., Geller, O., Amariglio, N., Simon, A. J., Rechavi, G., and Gal-Yam, E. N. (2005) *J. Cell Sci.* **118,** 4017–4025
58. Janicki, S. M., Tsukamoto, T., Salghetti, S. E., Tansey, W. P., Sachidanandam, R., Prasanth, K. V., Ried, T., Shav-Tal, Y., Bertrand, E., Singer, R. H., and Spector, D. L. (2004) *Cell* **116,** 683–698
59. Fischle, W., Wang, Y., and Allis, C. D. (2003) *Nature* **425,** 475–479